Available online at www.sciencedirect.com
SCIENCE DIRECT
Journal of Power Sources 153 (2006) 68–75
JOURNAL OF POWER SOURCES
www.elsevier.com/locate/jpowsour

Numerical study of a flat-tube high power density solid oxide fuel cell Part II: Cell performance and stack optimization

Yixin Lu [1], Laura Schaefer *

Department of Mechanical Engineering, University of Pittsburgh, Benedum Engineering Hall, Pittsburgh, PA 15261, USA

Received 11 February 2005; accepted 10 March 2005
Available online 31 May 2005

Abstract

The flat-tube high power density (HPD) solid oxide fuel cell (SOFC) is a geometry based on a tubular type SOFC, and is being developed by Siemens Westinghouse and other international companies in Japan and Korea. It has increased power density, but still maintains the beneficial feature of secure sealing for a tubular SOFC. In this paper, the electric performance of a flat-tube HPD SOFC is studied. This paper also investigates the effects of the stack chamber number, stack shape, and other stack geometry features on the performance of the flat-tube HPD SOFC. The results show that the performance of a flat-tube HPD SOFC is better than a tubular SOFC with the same active cell surface, and that increasing the number of chambers number can improve the overall performance of a flat-tube HPD SOFC. The height of a flat-tube HPD SOFC and the thickness of the ribs do not have much effect on the performance of the cell as is expected. This study will help to design and optimize the flat-tube HPD SOFC.

Keywords: Flat-tube; High power density (HPD); Solid oxide fuel cell (SOFC); Simulation; Performance; Optimization

1. Introduction

A solid oxide fuel cell (SOFC), like any other fuel cell, produces electrical power through an electrochemical reaction. Working at a high operating temperature (600–1000 °C), SOFCs are clean, quiet, and highly efficient power generation devices, and are now considered to be one of the most promising stationary power generating methods for the future [1–3].

There are currently two major types of SOFCs, planar and tubular. In a planar SOFC, the major components are a cathode, an anode, an electrolyte, and an interconnection. The components are all laminated in a plate-type structure (Fig. 1). The major advantages of a planar SOFC are manufacturing ease and high current density.

The tubular SOFC design is another major type of SOFC. It consists of the same components as a planar SOFC, namely a cathode, an anode, an electrolyte, and an interconnect, but in a different structure, as seen in Fig. 2. Air and fuel are provided in the arrangement as shown in Fig. 3. Due to their geometry, tubular designs have a self-sealing structure, which improves thermal stability and eliminates the need for the highly thermal-resistant sealants that are required in the planar configuration.

Comparisons between the results of Singhal [1], Williams et al. [3], and Godfrey et al. [4] show that a tubular SOFC has a much lower current density than a planar SOFC. This is because of the in-plane path that the electrons must travel along the circumferential electrodes to the cell interconnect, which increases internal ohmic losses.

In the last 15 years, significant progress has been achieved in tubular SOFC development by Siemens Westinghouse. Some tubular SOFC demonstration units have been operated for increasing duration [5]. Currently, the biggest hurdle to the large-scale commercialization of tubular SOFCs is their rather high cost, so manufacturers are now concentrating on

* Corresponding author. Tel.: +1 412 624 9793; fax: +1 412 624 4846.
E-mail addresses: yil52002@yahoo.com (Y. Lu), laschaef@engr.pitt.edu (L. Schaefer).
[1] Tel.: +1 412 624 9766; fax: +1 412 624 4846.

0378-7753/$ – see front matter © 2005 Elsevier B.V. All rights reserved.
doi:10.1016/j.jpowsour.2005.03.189

Nomenclature

A	constant in Eq. (5), cross-sectional area of discretized material in Eq. (7) (m^2)
B	constant in Eq. (6)
e^-	electron
EMF	electromotive force (V)
F	Faraday's constant 96486.7 ($C\,mol^{-1}$)
ΔG°	standard Gibbs free energy change ($J\,mol^{-1}$)
H_2	hydrogen
H_2O	water
i	local current density ($mA\,cm^{-2}$)
i_l	constant in Eq. (6)
i_n	constant in Eqs. (5) and (6)
i_0	constant in Eq. (5)
I	local current (A)
l	length of discretized material (m)
O_2	oxygen
$O^=$	oxide ion
P	pressure (Pa)
r	resistance (Ω)
R	universal gas constant 8.31434 ($J\,(mol\,K)^{-1}$)
T	temperature (K)

Greek letters

η	irreversible polarization (V)
ρ	electric resistivity (Ω m)

Subscripts

a	activation polarization
c	concentration polarization
H_2	hydrogen
H_2O	water vapor
o	ohmic
O_2	oxygen

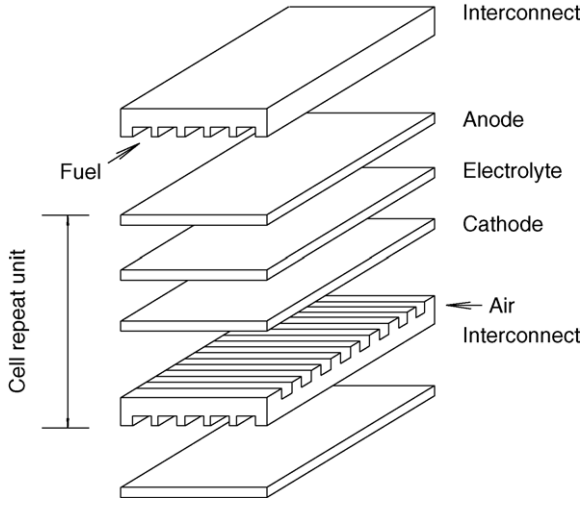

Fig. 1. Configuration of a planar SOFC.

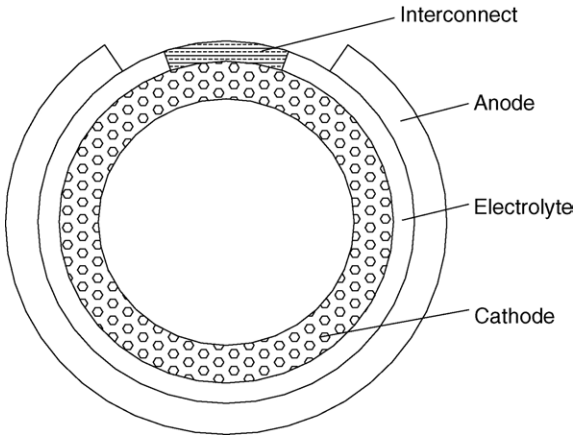

Fig. 2. Cross-section of a tubular SOFC.

reducing the overall cost of fuel cell-based power systems [3]. Efforts are being made to develop economically acceptable SOFC systems.

It is expected that the capital costs can be lowered through advancements in cell manufacturing and cell design. An increase in power density is considered to be one of the major technical contributions to further cut costs. So far, the research for increasing the power density has produced the cell design of a flat-tube high power density (HPD) SOFC. This design is expected to enhance the power density and yet retain the feature of secure sealing [6–8].

A flat-tube solid oxide fuel cell has the same components and working principles as that of a tubular solid oxide fuel cell. It is comprised of a cathode, an anode, an electrolyte, and an interconnect in a flat-tube structure as seen in Fig. 4.

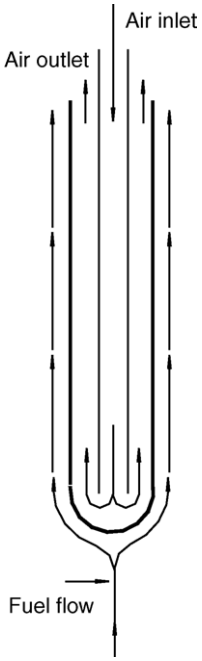

Fig. 3. Air and fuel delivery for a tubular SOFC.

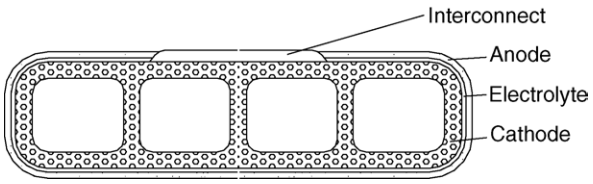

Fig. 4. Cross-section of a four-chamber flat-tube SOFC.

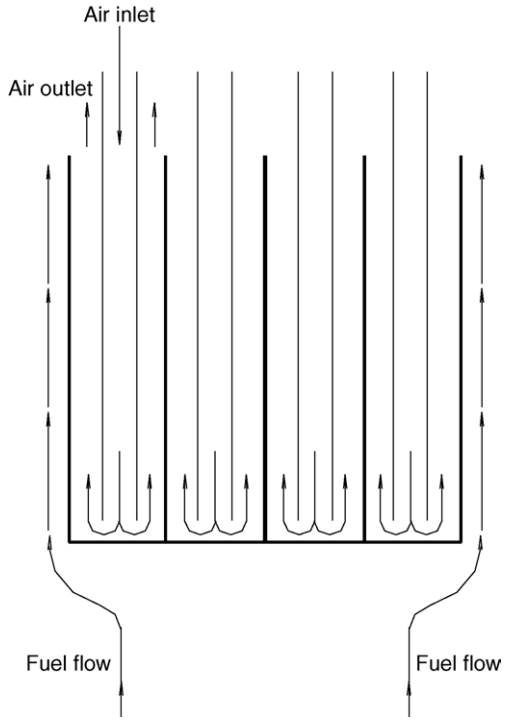

Fig. 5. Air and fuel flow arrangement for a four-chamber flat-tube SOFC.

The air and fuel delivery methods are also similar to that of a tubular SOFC (Fig. 5). Many flat-tube HPD SOFCs can be put together to form a bundle (Fig. 6).

The differences between a tubular solid oxide fuel cell and a flat-tube solid oxide fuel cell are the geometry and the structure of the cell stack. The cross-section of the flat-tube type SOFC looks like a flattened tube. Multiple ribs may be built into the cathode (air electrode) side, and the airflow area is divided into several chambers. Each chamber has its own air introducing tube. The number of chambers is decided by how many ribs are constructed. The ribs are electron conductive and can serve as a shortcut for the inner electron circuit, so that the electrons can flow not only circumferentially as in a tubular SOFC but also through these conductive ribs. This feature can reduce the cell resistance and hence increase the cell power density [6].

The flat-tube shape also makes it possible to keep the secure sealing feature of a tubular SOFC. Furthermore, since the internal ohmic resistance can be reduced by adding ribs into the cell stack, the cathode can be made thinner than before to decrease the concentration losses at the cathode side. This was not possible previously in order to keep the ohmic losses under a certain level. An additional benefit is that the void space between the cell stacks is reduced due to the cell stack geometry, and the cell bundle becomes more compact. Because of the features discussed above, this flat-tube configuration is expected to have an improved performance compared to the tubular SOFC.

Almost all of the current literature on SOFC simulations has focused exclusively on the planar or tubular configurations. In order to evaluate the potential for improved performance for flat-tube HPD SOFCs, simulations of both local properties and overall performance are needed. The current work described in this paper simulates the electric performance of a single HPD SOFC at steady state based on the previous research characterizing the thermal fluid properties of a flat-tube HPD SOFC [9]. The effects of the geometric features on the cell performance, such as rib number, rib thickness, cell stack shape, etc., are also studied.

2. Modeling

A solid oxide fuel cell basically consists of three major components, a porous air electrode (cathode), a porous fuel electrode (anode), and an electrolyte, which is gas tight but conductive to oxide ions. Oxygen at the cathode accepts the electrons from the external circuit to form oxide ions. The oxide ions conduct through the electrolyte to the anode–electrolyte interface and combine with the hydrogen to form water. The electrons released in this process flow through the external circuit back to the cathode.

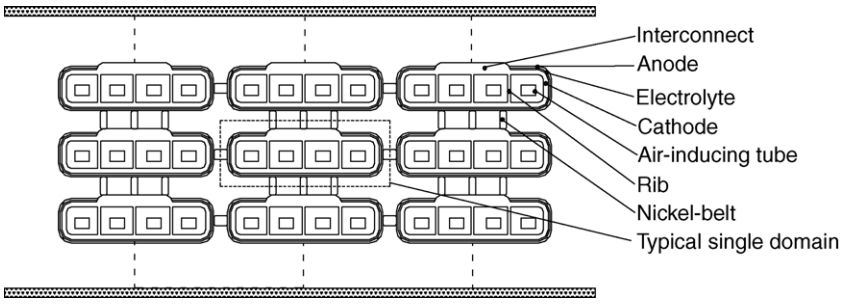

Fig. 6. Orientation of a flat-tube SOFC in a cell bundle.

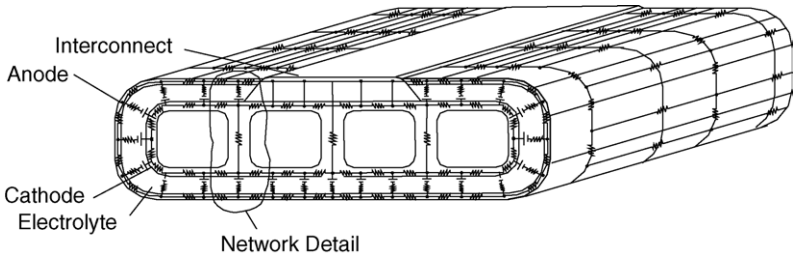

Fig. 7. Electric circuit network of a discretized cell stack.

The reactions in a hydrogen-consuming SOFC are:

$$\text{Cathode}: \quad \tfrac{1}{2}O_2 + 2e^- \Rightarrow O^= \tag{1}$$

$$\text{Anode}: \quad H_2 + O^= \Rightarrow H_2O + 2e^- \tag{2}$$

$$\text{Overall}: \quad H_2 + \tfrac{1}{2}O_2 \Rightarrow H_2O \tag{3}$$

The free energy change of the overall chemical reaction is converted to electrical energy via an electrical current. The electrical potential or the electromotive force (EMF) between the cathode and the anode is related to the change of the Gibbs free energy of the chemical reaction, the temperature T at the reaction site, and the partial pressures of the participating species through the well known Nernst equation:

$$\text{EMF} = \frac{-\Delta G^\circ_{H_2O}}{2F} + \frac{RT}{2F} \ln\left(\frac{p_{H_2} p_{O_2}^{1/2}}{p_{H_2O}}\right) \tag{4}$$

p_{H_2O} and p_{H_2} are the partial pressures of the water vapor and hydrogen at the anode–electrolyte interface, p_{O_2} the partial pressure of oxygen at the interface of the cathode and the electrolyte, T the temperature at the interface of the anode and the electrolyte, and $\Delta G^\circ_{H_2O}$ is the change of the standard Gibbs free energy of the electrochemical reaction, which is a function of the reaction temperature.

The SOFC output voltage is lower than the ideal voltage (EMF) due to the irreversibility of the reaction process. There are three major irreversible losses: activation, concentration, and ohmic losses. These losses are reflected by reductions in the voltage. The activation loss is described using the Tafel equation:

$$\eta_a = A \ln\left(\frac{i + i_n}{i_0}\right) \tag{5}$$

where i is local current density and i_n, i_0, and B are constants. The concentration loss is calculated by:

$$\eta_c = -B \ln\left(1 - \frac{i + i_n}{i_l}\right) \tag{6}$$

where i is local current density and i_n, i_l, and A are constants. The ohmic loss is described by Kirchhoff's law:

$$\eta_o = Ir \tag{7}$$

where r is the local resistance of the discretized material of the anode, electrolyte, and cathode, as shown in Figs. 7 and 8.

The SOFC output voltage, total current, and local voltage potentials can be determined by solving an electricity transmission circuit consisting of voltage sources and resistors, which is obtained by discretizing a SOFC stack. This method has been used by many researchers to predict the performances of many kinds of SOFCs [10–14]. The network circuit of the discretized cell stack of the flat-tube HPD SOFC is shown in Fig. 7. The detailed sample of the discretized network circuit near a rib is shown in Fig. 8. In the circuit network, the voltage sources are given by:

$$V = \text{EMF} - \eta_a - \eta_c \tag{8}$$

where EMF, η_a, and η_c are given by Eqs. (4)–(6), respectively. The ohmic losses η_o are distributed on the resistors in the electric circuit.

In the simulation, the EMFs are calculated based on the temperatures and pressures obtained in our previous work [9]. The constants for the irreversible losses are given in Table 1.

The local resistances of the discretized material of the anode, electrolyte, and cathode, as shown in Figs. 7 and 8, can be calculated by:

$$R = \rho \frac{l}{A} \tag{9}$$

where ρ is the resistivity of a material, l and A are the length and cross-sectional area of a discretized unit. For simplicity,

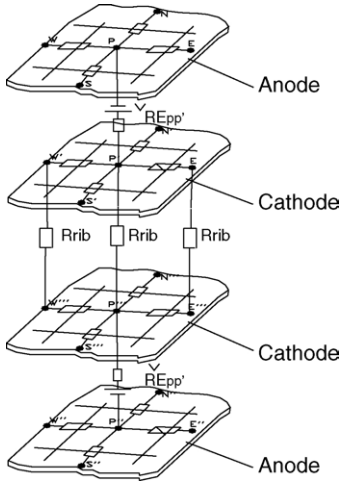

Fig. 8. Sample of the discretized network circuit near a rib (network detail in Fig. 7).

Table 1
Constants for Eqs. (5) and (6)

Constants for a high temperature SOFC	
A (V)	0.04
B (V)	0.002
i_n (mA cm^{-2})	2
i_0 (mA cm^{-2})	0.02
i_l (mA cm^{-2})	670

Table 2
Materials' conductivities of the HPD SOFCs [15]

Cathode resistivity (Ω cm)	0.013
Anode resistivity (Ω cm)	0.001
Electrolyte resistivity (Ω cm)	10
Interconnect resistivity (Ω cm)	0.6

in this study, the material conductivities of the anode, cathode, and electrolyte are assumed to be constants in the operating temperature range of 850–1000 °C. The conductivities of the electrodes and electrolyte are shown in Table 2.

Some basic dimensions of a flat-tube HPD SOFC are listed in Table 3. Other necessary dimensions can be calculated from the basic dimensions.

3. Results and discussions

In the simulation, the four-chamber flat-tube HPD SOFC is discretized to 400 units circumferentially and 5 units in length. To keep the discretization dimensions and simulations consistent, in Section 3.3, a cell stack with more chambers is discretized proportionally.

The temperature and pressure distributions of a flat-tube HPD SOFC are based on our former work [9]. In the geometric parameter effect analysis, the EMFs are calculated based on the temperature and concentration fields at a current density of 400 mA cm^{-2}.

The electricity transmission network (Fig. 7) is simulated using a commercial electric circuit analysis tool [16].

3.1. Result validation

Since the flat-tube SOFCs are developed based on the general manufacturing techniques used for tubular SOFCs, the base case for the flat-tube SOFC is assumed to utilize the same materials, and electrodes and electrolyte thicknesses.

Table 3
Flat-tube HPD SOFC dimensions in this simulation

Cell length (cm)	50
Cathode thickness (mm)	2.2
Electrolyte (μm)	40
Anode thickness (μm)	100
Interconnection thickness (μm)	85
Chamber width (cm)	1.5
Chamber height (cm)	1.5
Rib thickness (cm)	0.25

Table 4
Tubular SOFC dimensions and performance [5,6]

Cell length (cm)	150
Cell diameter (mm)	22
Cathode thickness (mm)	2.2
Electrolyte (μm)	40
Anode thickness (μm)	100
Interconnection thickness (μm)	85
Interconnection width (mm)	9
Active area (cm^2)	834

To validate the model developed to simulate the performance of a flat-tube HPD SOFC, a performance simulation of a 1.5-m long tubular SOFC, developed by Siemens Westinghouse, was conducted. The dimensions of this tubular SOFC are listed in Table 4.

The simulation result of the tubular SOFC is compared with performance data from the manufacturer [3], as shown in Fig. 9. We can see that the curves of terminal voltage versus current density and power versus current density agree well.

3.2. Single rib effect

To show how much effect a rib has on the performance of a tubular SOFC, a one-rib flat-tube HPD SOFC, which has the same active surface as that of a 0.5-m long tubular SOFC, is simulated. The comparisons of the terminal voltage and power output are demonstrated in Fig. 10. As can be clearly seen, the performance of a tubular SOFC is improved significantly by adding a rib to it. The terminal voltage increases in the whole range, which means that the internal ohmic resistance decreases as expected.

3.3. Multiple rib effect

Given that a single rib can improve SOFC performance, the question of how many ribs should be optionally constructed into a flat-tube HPD SOFC is very important. To

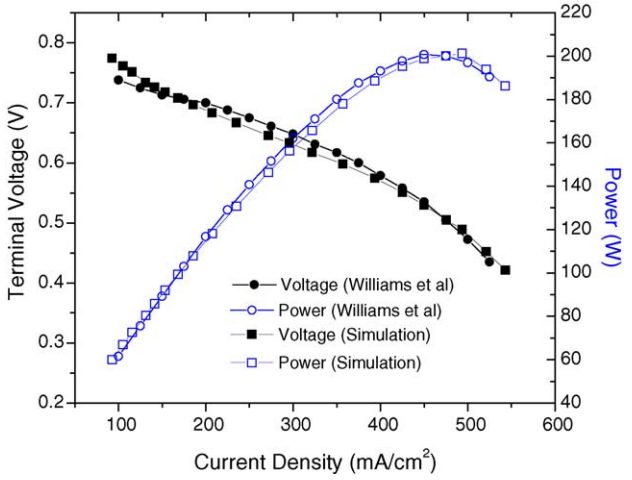

Fig. 9. Performance comparison between the simulation result and the performance data from manufacturer of a 1.5-m long SOFC.

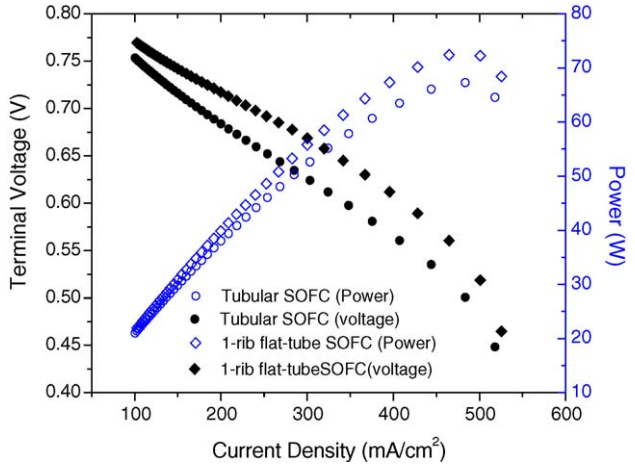

Fig. 10. Performance comparison between a 0.5-m long tubular SOFC and a one-rib flat-tube SOFC with same active surface.

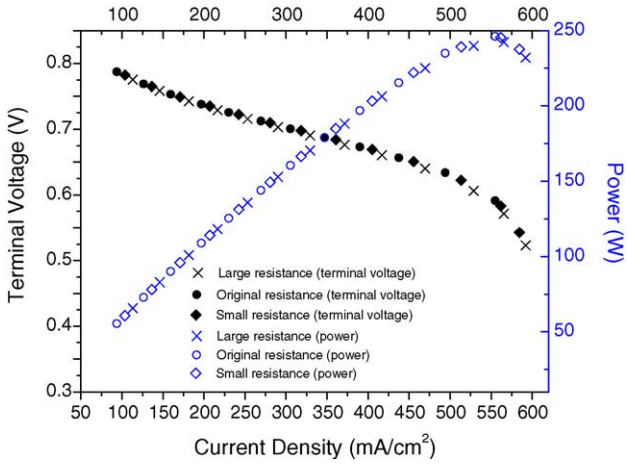

Fig. 12. Performance comparisons of flat-tube SOFCs with different rib resistances.

find the performance of flat-tube SOFCs with different numbers of ribs, example flat-tube HPD SOFCs with 3, 7, and 15 ribs are presented for comparison. The terminal voltage and power output curves are plotted in Fig. 11.

From Fig. 11, we can see that increased rib number can improve the terminal voltage. However, the terminal voltage improvement from an 8-chamber (7-rib) case to a 16-chamber (15-rib) case is far less than from a 4-chamber (3-rib) to the 8-chamber case. In other words, the impact of the rib number on the terminal voltage is significant only when the rib number is not too big. The effect decreases with the increasing rib number. Additionally, at low current density (for example, less than 200 mA cm^{-2}), this rib number has only a negligible impact on the terminal voltage. Fig. 11 also shows that the power output is almost proportional to the rib number because the increased rib number directly increases the active surface of a flat-tube SOFC. Through studying the SOFC performance variation with the rib number, when the rib number is larger, it is expected that while increasing the rib number further will improve the terminal voltage little, it will improve the power/volume rating.

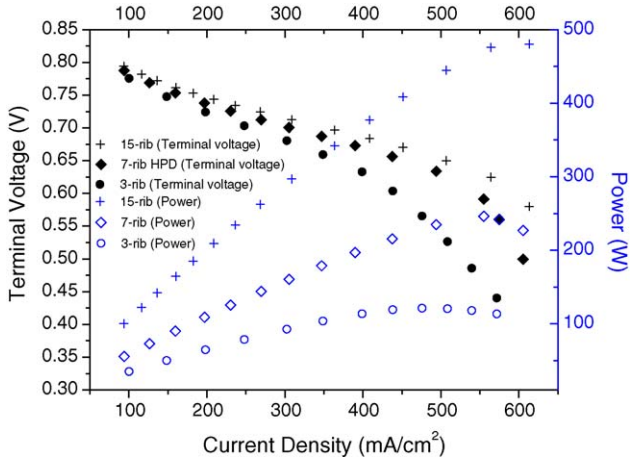

Fig. 11. Performance comparisons of flat-tube SOFCs with 3, 7, and 15 ribs.

3.4. Effect of rib resistance

In this study, the same material and porosity are used for the ribs as for the cathode in the cell tube. To find out the effect of the rib resistance on the cell performance, two additional cases, in which rib resistances have been modified based on the seven-rib (eight chambers) flat-tube HPD SOFC, are studied. The first case is a seven-rib flat-tube SOFC, which has a doubled rib resistance compared the original one. The second case is when the rib resistance is reduced by half. The simulation results are plotted in Fig. 12.

From Fig. 12, we can conclude that when the ribs are constructed with the same material, porosity, and thickness as the cathode, modification of the rib resistance by, for example, increasing or decreasing the rib thickness or making the cell stack more flattened will not have a significant effect on the flat-tube SOFC performance. The reason for this result is that the resistance of the rib is much less than the circumferential resistance, so the proposed variations will affect the circuit performance only negligibly.

3.5. Effect of interconnect resistance

To discover the effect of the interconnect resistance on the performance of the flat-tube HPD SOFC, two cases are studied based on a seven-rib (eight chambers) flat-tube SOFC. In one case, the interconnect resistance is original, whereas in the other case, we adopt a certain interconnect resistance which gives rise to the same effect as if we applied three layers of the original interconnect on the anode. This performance comparison is shown in Fig. 13.

From Fig. 13, we can determine that the interconnect resistance does indeed have a significant impact on the performance. Increasing the interconnect resistance will decrease the performance of the SOFC. This is because adding a little

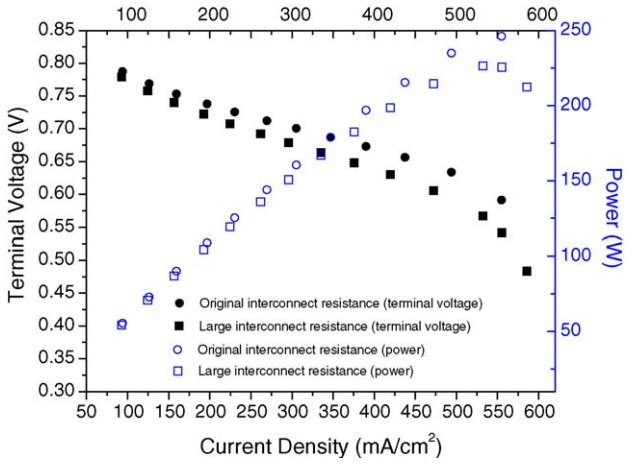

Fig. 13. Performance comparisons of flat-tube SOFCs with different interconnect resistances.

resistance to the interconnect will affect the resistance of the entire circuit significantly.

3.6. Effect of cathode thickness

As mentioned in Section 1, since the internal ohmic resistance can be reduced by adding ribs into the cell stack, it is possible that we can make the cathode thinner to decrease the concentration loss at the cathode side, which could not be done before in order to keep the ohmic losses under a certain level. A case in which the cathode thickness of a flat-tube HPD SOFC with seven ribs was changed from 2.2 to 1.5 cm was studied. The performance comparisons between the original HPD SOFC and the HPD SOFC with a thinner cathode are shown in Fig. 14. The result shows that the cathode thickness has no significant effect on the performance of the HPD SOFC. Making the cathode thinner to reduce the concentration loss may be beneficial for the fuel cell performance.

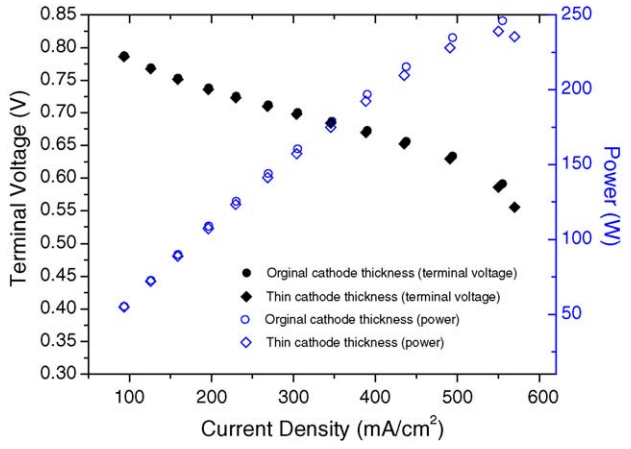

Fig. 14. Performance effects of the HPD SOFCs with different cathode thicknesses.

4. Conclusions

Solid oxide fuel cells are in the process of commercialization, but the manufacturing costs need to be further reduced, which can be achieved through improved performance and proven reliability. The flat-tube HPD SOFCs are expected to improve the performance of tubular SOFCs while maintaining secure sealing and high durability. The goal of this research is to simulate the electric performance of a flat-tube HPD SOFC and study the effects of rib number, dimensions, material conductivities, and cell stack structure on cell performance.

The number of ribs has a positive effect on the cell performance. An increased rib number will improve the cell terminal voltage. The improvement is greater when the rib number is increased from a small to a median value. However, further increasing the rib number will decrease the magnitude of the improvement. The power output is almost proportional to the active surface, so the power produced will directly increase with the rib number. When a flat-tube HPD SOFC has many chambers (for example, 16), further increasing the rib number may not increase the terminal voltage significantly, but will improve the power/volume rating.

If the cathode material is used for the ribs, and the thickness of the ribs is in the range of 1–4 mm, making the rib thicker or making the cell tube into a more flattened shape to decrease the rib resistance will not have a significant effect on the performance. On the other hand, a more flattened shape will improve the power/volume rating.

The interconnect material conductivity has a significant impact on the cell performance. To improve the performance, the interconnect must have a low resistance and a good contact with the cell stack to reduce the contact resistance.

Additionally, making the cathode thinner has the potential to reduce the concentration loss and improve the overall fuel cell performance.

References

[1] S.C. Singhal, Solid State Ionics 152–153 (2002) 405–410.
[2] A.B. Stambouli, E. Traversa, Renewable Sustainable Energy Rev. 6 (2002) 433–455.
[3] M.C. Williams, J.P. Strakey, S.C. Singhal, J. Power Sources 131 (2004) 79–85.
[4] B. Godfrey, K. Föger, R. Gillespie, R. Bolden, S.P.S. Badwal, J. Power Sources 86 (2000) 68–73.
[5] R.A. George, J. Power Sources 86 (2000) 134–139.
[6] S.C. Singhal, Solid State Ionics 135 (2000) 305–313.
[7] N.F. Bessette, B.P. Borglum, H. Schichl, D.S. Schmidt, Power J. (Magazine of the Siemens Power Generation Group), January 2001, pp. 10–13.
[8] S.D. Vora, D. Collins, Fuel Cell Annual Report, 2003, pp. 18–20.
[9] Y. Lu, L. Schaefer, P. Li, J. Power Sources 140 (2005) 331–339.
[10] K. Takano, S. Nagata, K. Nozaki, A. Monma, T. Kato, Y. Kaga, A. Negishi, K. Kato, T. Inagaki, H. Yoshida, et al., J. Power Sources 132 (2004) 42–51.
[11] P.W. Li, M.K. Chyu, J. Power Sources 124 (2003) 487–498.

[12] M. Iwata, T. Hikosaka, M. Morita, T. Iwanari, K. Ito, K. Onda, Y. Esaki, Y. Sakaki, S. Nagata, Solid State Ionics 132 (2000) 297–308.
[13] A. Hirano, M. Suzuki, M. Ipponmatsu, J. Electrochem. Soc. 139 (1992) 2744–2751.
[14] E.F. Sverdrup, C.J. Warde, R.L. Eback, Energy Convers. 13 (1973) 129–136.
[15] N.F. Bessette, W.J. Wepfer, J. Energy Resour. Technol. 117 (1995) 43–49.
[16] Ansoft Corporation, http://www.ansoft.com.